AMERICAN SOCIETY FOR MICROBIOLOGY | Molecular and Cellular Biology®

RESEARCH ARTICLE

# NFE2L1 and NFE2L3 Complementarily Maintain Basal Proteasome Activity in Cancer Cells through CPEB3-Mediated Translational Repression

**Tsuyoshi Waku,[a] Hiroyuki Katayama,[b] Miyako Hiraoka,[b] Atsushi Hatanaka,[b,c] Nanami Nakamura,[b] Yuya Tanaka,[a] Natsuko Tamura,[b] Akira Watanabe,[d] Akira Kobayashi[a,b]**

[a]Laboratory for Genetic Code, Department of Medical Life Systems, Faculty of Life and Medical Sciences, Doshisha University, Kyotanabe, Kyoto, Japan
[b]Laboratory for Genetic Code, Graduate School of Life and Medical Sciences, Doshisha University, Kyotanabe, Kyoto, Japan
[c]Research Fellow of Japan Society for the Promotion of Science, Tokyo, Japan
[d]Department of Life Science Frontiers, Center for iPS Cell Research and Application, Kyoto University, Kyoto, Japan

Tsuyoshi Waku and Hiroyuki Katayama contributed equally to this work. Author order was determined by the time spent on the project and in order of increasing seniority.

**ABSTRACT** Proteasomes are protease complexes essential for cellular homeostasis, and their activity is crucial for cancer cell growth. However, the mechanism of how proteasome activity is maintained in cancer cells has remained unclear. The CNC family transcription factor NFE2L1 induces the expression of almost all proteasome-related genes under proteasome inhibition. Both *NFE2L1* and its phylogenetically closest homolog, *NFE2L3*, are highly expressed in several types of cancer, such as colorectal cancer. Here, we demonstrate that NFE2L1 and NFE2L3 complementarily maintain basal proteasome activity in cancer cells. Double knockdown of *NFE2L1* and *NFE2L3* impaired basal proteasome activity in cancer cells and cancer cell resistance to a proteasome inhibitor anticancer drug, bortezomib, by significantly reducing the basal expression of seven proteasome-related genes: *PSMB3*, *PSMB7*, *PSMC2*, *PSMD3*, *PSMG2*, *PSMG3*, and *POMP*. Interestingly, the molecular basis behind these cellular consequences was that NFE2L3 repressed NFE2L1 translation by the induction of the gene encoding the translational regulator CPEB3, which binds to the *NFE2L1* 3′ untranslated region and decreases polysome formation on *NFE2L1* mRNA. Consistent results were obtained from clinical analysis, wherein patients with cancer having tumors expressing higher levels of *CPEB3*/*NFE2L3* exhibit poor prognosis. These results provide the novel regulatory mechanism of basal proteasome activity in cancer cells through an NFE2L3-CPEB3-NFE2L1 translational repression axis.

**KEYWORDS** CPEB3, NFE2L1, NFE2L3, NRF1, NRF3, colorectal cancer, proteasome, translation

Cancer cell survival and growth are dependent on the activity of proteasomes, which are large protease complexes that catalyze the precise and rapid degradation of proteins involved in antitumorigenic events, such as cell cycle arrest and apoptosis induction (1, 2). One of the proteasome regulators in mammals is the cap'n'collar (CNC) family transcription factor NFE2L1 (nuclear factor erythroid-2-like 1; NRF1). NFE2L1 induces the expression of almost all proteasome-related genes under proteasome inhibition (3–6), and its brain-specific knockout actually impairs proteasome function and causes neurodegeneration in mice (7). However, the transcriptional regulation of proteasome activity in cancer cells has remained unclear.

Phylogenetically, NFE2L3 (nuclear factor erythroid-2-like 3; NRF3) has been identified as the closest homolog of NFE2L1 in the CNC family (8). Recently, *NFE2L3* gene amplification has been reported in patients with colorectal cancer (9). On the

**Citation** Waku T, Katayama H, Hiraoka M, Hatanaka A, Nakamura N, Tanaka Y, Tamura N, Watanabe A, Kobayashi A. 2020. NFE2L1 and NFE2L3 complementarily maintain basal proteasome activity in cancer cells through CPEB3-mediated translational repression. Mol Cell Biol 40:e00010-20. https://doi.org/10.1128/MCB.00010-20.



Address correspondence to Akira Kobayashi, akobayas@mail.doshisha.ac.jp.

**Received** 9 January 2020
**Returned for modification** 16 February 2020
**Accepted** 27 April 2020
**Accepted manuscript posted online** 4 May 2020
**Published** 29 June 2020

Gene Expression Profiling Interactive Analysis (GEPIA) Web server (10), the *NFE2L3* gene is shown to be highly expressed in many types of tumors, such as testicular germ cell tumors, pancreatic adenocarcinoma, colon adenocarcinoma (COAD), and rectal adenocarcinoma (READ), whereas the *NFE2L1* gene is highly expressed in almost all types of normal and tumor tissue. These insights imply the functional correlation between NFE2L1 and NFE2L3 with respect to the maintenance of basal proteasome activity in cancer cells.

In this study, we show that both NFE2L1 and NFE2L3 are required to maintain basal proteasome activity in cancer cells through inducing the expression of several proteasome-related genes, including *PSMB3*, *PSMB7*, *PSMC2*, *PSMD3*, *PSMG2*, *PSMG3*, and *POMP*. Interestingly, NFE2L3 represses NFE2L1 translation by inhibiting polysome formation on *NFE2L1* mRNA. We identify a translational regulator, *CPEB3* (*cytoplasmic polyadenylation element-binding protein 3*), as an NFE2L3 target gene that is involved in the repression of NFE2L1 translation. A functional CPEB recognition motif is also identified in the *NFE2L1* 3′ untranslated region (*NFE2L1*-3′UTR). Furthermore, we confirm that CPEB3 is a key factor for not only the complementary maintenance of basal proteasome activity by NFE2L1 and NFE2L3 but also the poor prognosis of colorectal cancer patients, with tumors highly expressing *NFE2L3* but not *NFE2L1*. In conclusion, we demonstrate the novel regulatory mechanism of basal proteasome activity in cancer cells where NFE2L1 and NFE2L3 complementarily, but not simultaneously, maintain the basal expression of proteasome-related genes through CPEB3-mediated translational repression.

## RESULTS

**Both NFE2L1 and NFE2L3 are required to maintain basal proteasome activity in cancer cells.** Initially, we investigated the biological relevance of NFE2L1 and NFE2L3 for proteasome activity at the basal level in living cancer cells. Using human colorectal carcinoma HCT116 cells, we generated cells that stably expressed the ZsProSensor-1 fusion protein, a proteasome-sensitive fluorescent reporter (see Fig. S1A in the supplemental material). Once the proteasome in this stable cell line was inhibited by proteasome inhibitor MG-132, green fluorescence derived from the reporter protein was detected using a flow cytometer (Fig. S1B). We found that the double knockdown of *NFE2L1* and *NFE2L3* significantly decreased basal proteasome activity in living cancer cells (Fig. 1A). Consistent results were obtained by *in vitro* proteasome activity assays (Fig. S1C). The double knockdown also impaired the resistance of cancer cells to a proteasome inhibitor, bortezomib (BTZ), which is clinically used as an anticancer drug (11, 12) (Fig. 1B).

We next investigated the impact of NFE2L1 and NFE2L3 on the expression of proteasome-related genes. To address this issue, we performed DNA microarray analysis using *NFE2L1* or *NFE2L3* knockdown HCT116 cells and found 42 proteasome-related genes with a decrease in expression to less than 0.7-fold (Table S1). Gene set enrichment analysis (GSEA) using these array data sets showed reduced expression of 17 common core genes in both *NFE2L1* and *NFE2L3* knockdown cells (Fig. S1D and E and Table S2). Therefore, using reverse transcription-quantitative PCR (RT-qPCR), we showed that the mRNA levels of *PSMB3*, *PSMB7*, *PSMC2*, *PSMD3*, *PSMG2*, *PSMG3*, and *POMP* were significantly decreased by the double knockdown of *NFE2L1* and *NFE2L3* (Fig. 1C). These results indicate that both NFE2L1 and NFE2L3 are required to maintain the basal expression of several proteasome-related genes. We obtained similar results using other cancer cell lines, including T98G (human glioblastoma multiforme) and MCF-7 (human breast cancer) (Fig. S1F and G).

NFE2L1 induces the expression of proteasome-related genes by directly binding antioxidant response elements (ARE) in their promoters (3–6). NFE2L3 also binds to ARE sequences *in vitro* (8), although it has not been reported whether it binds to the ARE in the promoters of proteasome-related genes in cells. To address this issue, we analyzed our chromatin immunoprecipitation (ChIP) sequencing data sets in the presence of proteasome inhibitor MG-132, which stabilizes both NFE2L1 and NFE2L3

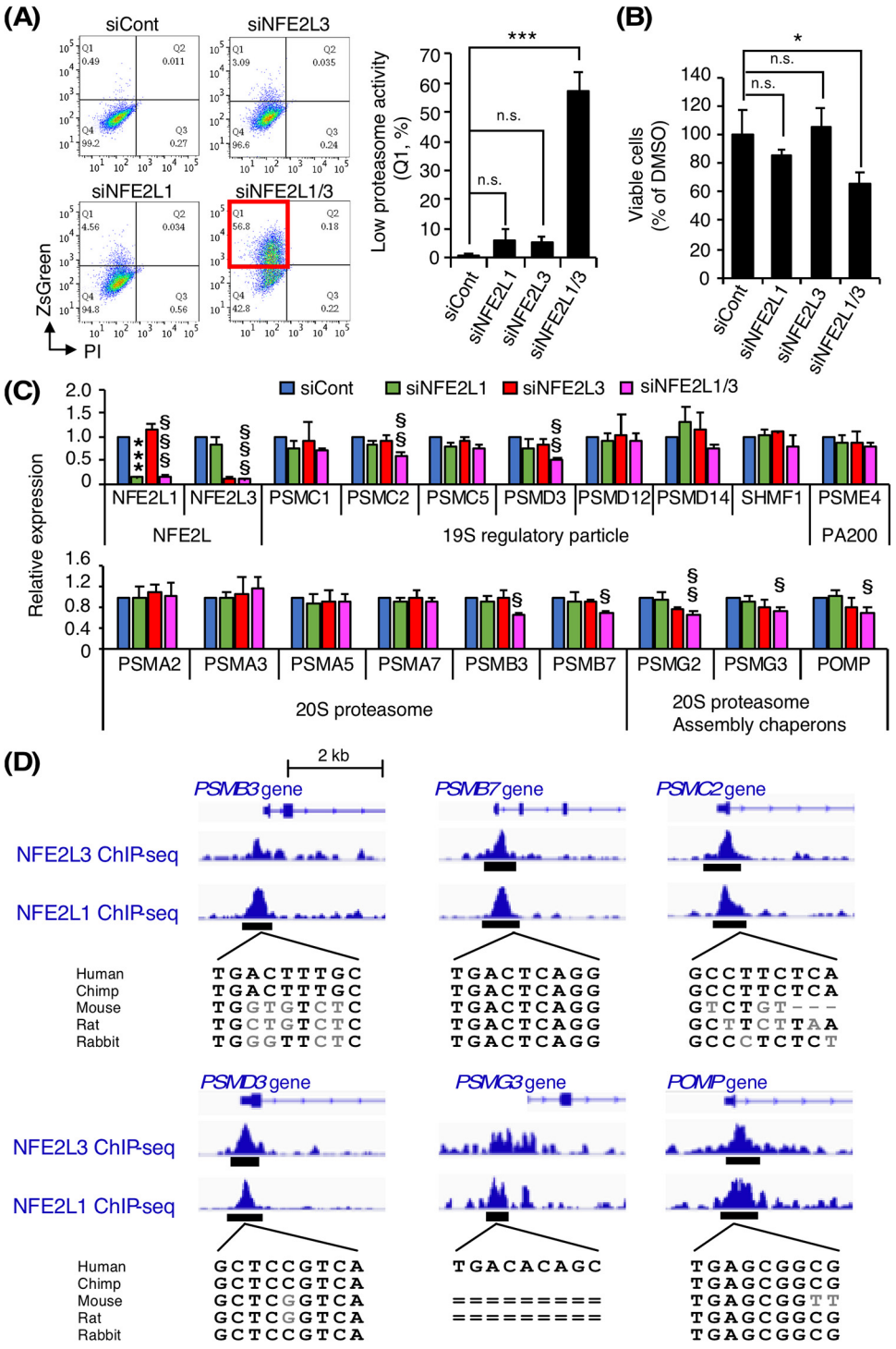


**FIG 1** NFE2L1 and NFE2L3 complementarily regulate proteasome activity and proteasome subunit gene expression at the basal level. (A) Impact of *NFE2L* knockdown on basal proteasome activity. At 24 h after siRNA transfection into ZsPS cells, the fluorescence intensity derived from a ZsProSensor-1 reporter was measured using flow cytometry. The cell populations in Q1 enclosed by a red line are those with low proteasome activity. siNFE2L1/3 represents the double knockdown of *NFE2L1* and *NFE2L3*. Control siRNA (siCont) was used as a control. ***, $P < 0.005$; n.s., not significant ($n = 3$, means + SD, ANOVA followed by Tukey's test). (B) Impact of *NFE2L* knockdown on BTZ resistance. At 24 h after siRNA transfection into HCT116 cells, the cells were treated with 5 nM BTZ and further incubated for 48 h. The cells then were subjected to cell viability assay using trypan blue staining. siNFE2L1/3 represents the double knockdown of *NFE2L1* and *NFE2L3*. Control siRNA (siCont) and dimethyl sulfoxide (DMSO) were used as controls. Cell viability was determined by the number of living cells with BTZ treatment normalized by that with DMSO. *, $P < 0.05$; n.s., not significant ($n = 3$, means + SD, ANOVA followed by Tukey's test). (C) Impact of *NFE2L* knockdown on mRNA levels of 17 common core genes with a "yes" value in core

(Continued on next page)

proteins (our unpublished data), and found positive ChIP peaks of NFE2L1 and NFE2L3 proteins on the promoters of *PSMB3*, *PSMB7*, *PSMC2*, *PSMD3*, *PSMG3*, and *POMP* genes (Fig. 1D), suggesting that NFE2L3 as well as NFE2L1 directly induces the basal expression of several proteasome-related genes.

**NFE2L3 represses NFE2L1 translation by inhibiting polysome formation on *NFE2L1* mRNA.** To clarify the molecular mechanism behind the maintenance of basal proteasome activity in cancer cells by both NFE2L1 and NFE2L3, we investigated the relationship between NFE2L1 and NFE2L3 expression in HCT116 cells. Interestingly, NFE2L1 protein levels were increased by *NFE2L3*, knockdown, while NFE2L3 protein levels were not changed by *NFE2L1* knockdown (Fig. 2A). Multiple immunoblot bands of NFE2L1 and NFE2L3 proteins indicated distinct forms with protein processing mediated by an aspartic protease, DDI2 (DNA damage-inducible 1 homolog 2) (13, 14). Similar results were obtained in other cancer cell lines, including T98G and MCF-7 (Fig. S2A). The levels of *NFE2L1* mRNA were unchanged by *NFE2L3* knockdown (Fig. 2B and Fig. S2B). We also obtained consistent results in cells in which *NFE2L3* was overexpressed (Fig. S2C and D). On the other hand, the activation of NFE2L2 (nuclear factor erythroid-2-like 2; NRF2) by diethyl maleate (DEM) did not affect the protein and mRNA levels of NFE2L1 as well as NFE2L3 (Fig. S2E and F). These results indicate that NFE2L3 decreases NFE2L1 protein levels without altering *NFE2L1* gene expression, suggesting an effect of NFE2L3 on the protein stability or translation of NFE2L1. To investigate the former effect, we performed a cycloheximide (CHX) chase experiment and found that *NFE2L3* knockdown did not stabilize NFE2L1 proteins (Fig. 2C). Meanwhile, we investigated the latter effect by polysome profiling analysis and showed that *NFE2L3* knockdown increased the amount of *NFE2L1* mRNA in polysomes between fractions 11 and 20 (Fig. 2D), although rRNA distribution and global protein synthesis remained unchanged (Fig. S2G and H). These results indicate that NFE2L3 decreases polysome formation on *NFE2L1* mRNA, thereby repressing NFE2L1 translation. We further confirmed the increase of NFE2L1 recruitment onto the promoters of proteasome subunit genes by *NFE2L3* knockdown (Fig. S2I), implying that NFE2L1 induces the expression of proteasome subunit genes if *NFE2L3* expression is reduced.

**NFE2L3 directly induces the gene expression of translational regulator *CPEB3*.** To identify an NFE2L3 target gene that represses NFE2L1 translation, we performed DNA microarray analysis using *NFE2L3* knockdown HCT116 cells and *NFE2L3*-overexpressing H1299 (human non-small-cell lung cancer) cells; we identified 146 genes whose expression was positively associated with *NFE2L3* gene expression (Fig. S3A). Among these genes, we found *CPEB3* to be a candidate gene related to translational regulation, using gene ontology analysis (Fig. S3B), and confirmed this result using RT-qPCR (Fig. 3A). We then confirmed that NFE2L3 proteins bound to one of two ARE regions within the *CPEB3* promoter (Fig. 3B and C), indicating that NFE2L3 directly induces *CPEB3* gene expression. We investigated whether CPEB3 is related to the NFE2L3-mediated regulation of NFE2L1 translation and found that *CPEB3* knockdown increased NFE2L1 protein levels and the amount of *NFE2L1* mRNA in polysomes, while the rRNA distribution and global protein synthesis remained unchanged (Fig. 3D and E and Fig. S3C to E). We further confirmed that NFE2L1 protein levels were decreased by *CPEB3* overexpression (Fig. 3F and Fig. S3F). These results clearly demonstrate that NFE2L3 specifically represses NFE2L1 translation in a CPEB3-dependent manner. We also found evidence of *CPEB3* gene induction by NFE2L1 (Fig. S3G), suggesting the

**FIG 1** Legend (Continued)
enrichment in both *NFE2L1* and *NFE2L3* knockdown cells (Table S2). At 48 h after siRNA transfection into HCT116 cells, the cells were analyzed by RT-qPCR. siNFE2L1/3 represents double knockdown of *NFE2L1* and *NFE2L3*. Control siRNA (siCont) was used as a control. mRNA levels of each proteasome subunit were normalized according to levels of *β-actin* mRNA ($n = 3$, mean + SD, ANOVA followed by Tukey's test; *, siCont versus siNFE2L1; †, siCont versus siNFE2L3; §, siCont versus siNFE2L1/3). (D) ChIP peaks of NFE2L1 and NFE2L3 in the promoters of proteasome-related genes. ChIP sequencing of endogenous NFE2L1 or exogenous NFE2L3 was performed using wild-type HCT116 cells or *NFE2L3*-overexpressing H1299 cells treated with 1 $\mu$M MG-132 for 24 h.

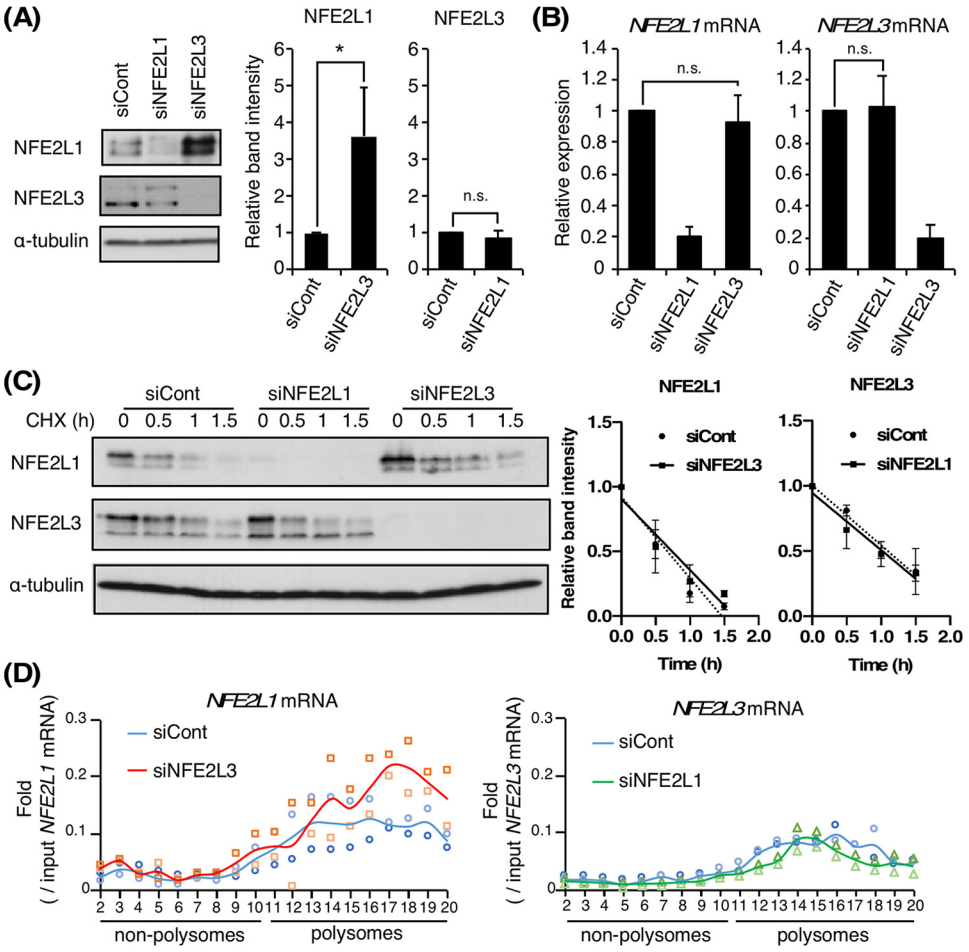


**FIG 2** NFE2L3 represses NFE2L1 translation by inhibiting polysome formation on *NFE2L1* mRNA. (A and B) Impact of *NFE2L* knockdown on protein and mRNA levels of another NFE2L in HCT116 (colorectal carcinoma) cells. At 48 h after siRNA transfection, the cells were analyzed by immunoblotting (A) and RT-qPCR (B). Protein or mRNA levels of each NFE2L were normalized with reference to $\alpha$-tubulin protein or *β-actin* mRNA, respectively. Control siRNA (siCont) was used as a control. *, $P < 0.05$; n.s., not significant ($n = 3$, means + SD; *t* test in panel A, ANOVA followed by Tukey's test in panel B). (C) Impact of *NFE2L* knockdown on protein degradation of another NFE2L. At 48 h after siRNA transfection, the cells were treated with CHX and analyzed by immunoblotting at the times indicated. Protein levels were normalized by $\alpha$-tubulin. Control siRNA (siCont) was used as a control ($n = 3$, means + SD). (D) Distribution of *NFE2L* mRNA in HCT116 transfected with the indicated siRNA ($n = 2$). At 48 h after siRNA transfection, the cells were analyzed by sucrose gradient centrifugation followed by RT-qPCR. mRNA levels in each fraction were normalized against those in the input. Mean and individual values are represented as a line and mark, respectively. Control siRNA (siCont) was used as a control.

presence of negative feedback regulation of NFE2L1 through CPEB3-mediated translational repression. We discuss the biological implications of this finding in Discussion.

Members of the CPEB family, as RNA-binding proteins, are essential regulators of posttranscriptional gene expression, with functions including the polyadenylation of 3′UTRs and ribosome recruitment onto mRNA (15). CPEB proteins recognize a pentanucleotide RNA sequence (5′-UUUUA-3′) in the 3′UTR of a target gene (16). Five CPEB recognition motifs (CPEs) are found in the *NFE2L1*-3′UTR (numbers highlighted in red in Fig. S3H). To identify the functional CPE, using an RNA immunoprecipitation (RIP) assay, we initially checked that *NFE2L1* mRNA was precipitated with transiently expressed 3×Flag-CPEB3 proteins (Fig. 3G). We next confirmed that *NFE2L3* knockdown induced the translation via *NFE2L1*-3′UTR (Fig. 3H) using a translational assay with a luciferase reporter and also obtained results consistent with those of the *CPEB3* knockdown (Fig. 3I). Finally, we performed deletion and mutation analysis using this translational assay (Fig. 3J). The deletion of the *NFE2L1*-3′UTR region containing CPE#2 to CPE#5 induced more translation than the full length, although the CPE#3 to CPE#5

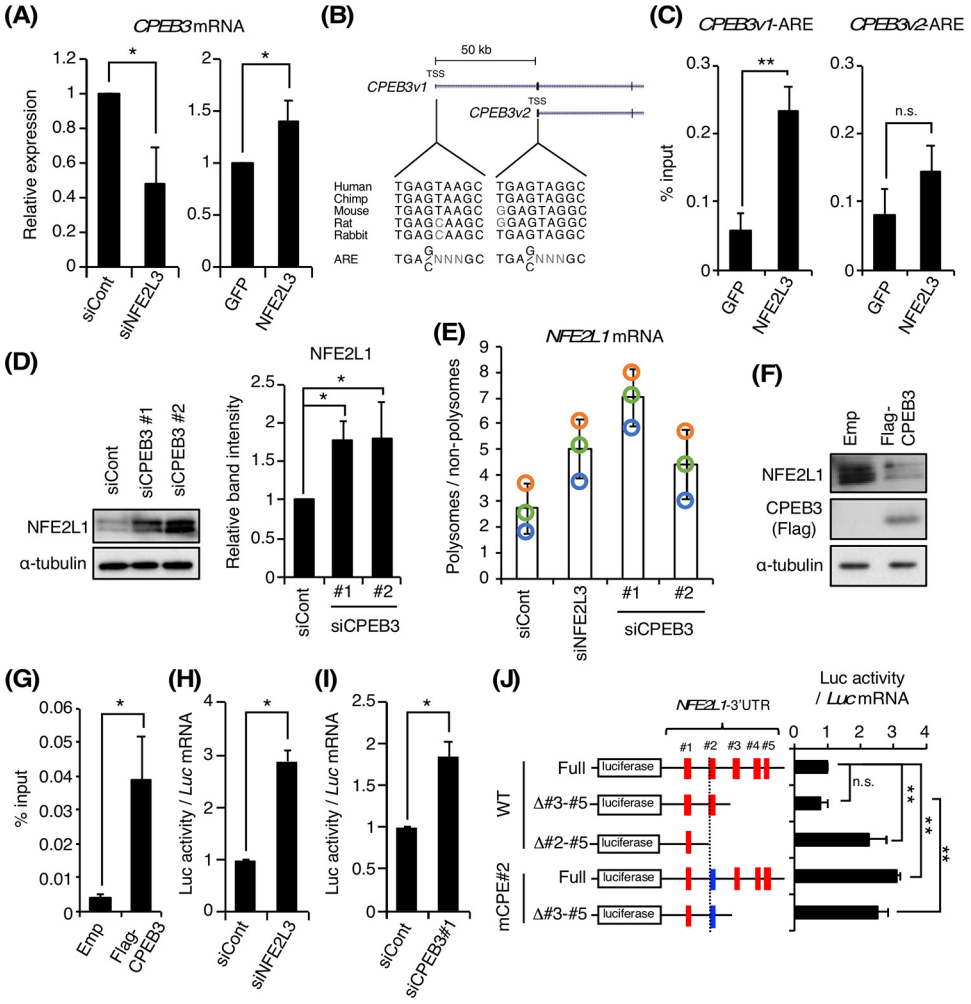


**FIG 3** CPEB3 is an NFE2L3 target gene that negatively regulates NFE2L1 translation. (A) Impact of *NFE2L3* knockdown on mRNA levels of *CPEB3* in HCT116 cells (left) and *NFE2L3*-overexpressing H1299 cells (right). Control siRNA (siCont) or *GFP*-overexpressing H1299 cells were used as controls. mRNA levels of *CPEB3* were normalized according to *β-actin* mRNA. *, $P < 0.05$ ($n = 3$, means + SD, *t* test). (B and C) The recruitment of NFE2L3 on *CPEB3* promoters in *NFE2L3*-overexpressing H1299 cells. *GFP*-overexpressing H1299 cells were used as controls. In panel B, the genome locus of the *CPEB3* promoter and multiple sequences of two candidate AREs in the indicated species are shown. TSS, transcription start site. **, $P < 0.01$; n.s., not significant ($n = 3$, means + SD, *t* test). (D) Impact of *CPEB3* knockdown on NFE2L1 protein levels. Each siRNA was transfected into HCT116 cells. After 48 h, the cells were analyzed by immunoblotting. Representative images of immunoblotting are shown in the left panel, and the protein levels were normalized by α-tubulin in the right panel. Control siRNA (siCont) was used as a control. *, $P < 0.05$ ($n = 3$, means + SD, ANOVA followed by Tukey's test). (E) Impact of *CPEB3* knockdown on the amount of *NFE2L1* mRNA on polysomes. At 48 h after siRNA transfection, the cells were subjected to sucrose gradient centrifugation. Fractions 2 to 8 and 11 to 19, shown in Fig. S3D, were collected as the nonpolysomal and polysomal fractions, respectively. Each fraction was analyzed by RT-qPCR. mRNA levels of *NFE2L1* in each fraction were normalized against those in the input. *NFE2L1* mRNA levels in the polysomal fractions then were divided by *NFE2L1* mRNA levels in the nonpolysomal fractions. Control siRNA (siCont) and siNFE2L3 were used as controls. Means + SD and three independent values are represented as bars and indicated colored marks, respectively ($n = 3$). (F) Impact of *CPEB3* overexpression on NFE2L1 protein levels. At 48 h after 3×Flag-CPEB3 plasmid transfection into HCT116 cells, the cells were analyzed by immunoblotting. p3×FLAG-CMV 10 vector without any fusion proteins was used as a control empty vector (Emp). (G) Interactions between CPEB3 protein and *NFE2L1* mRNA. At 24 h after 3×Flag-CPEB3 plasmid transfection, cells were analyzed by RIP assay followed by RT-qPCR. RNA immunoprecipitated mRNA levels of *NFE2L1* were normalized against the input values. p3×FLAG-CMV 10 vector without any fusion proteins was used as a control empty vector (Emp). *, $P < 0.05$ ($n = 3$, means + SD, *t* test). (H and I) Impact of *NFE2L3* or *CPEB3* knockdown on NFE2L1 translation via its 3′UTR. At 24 h after the transfection of siNFE2L3 (H) or siCPEB3 (I), a luciferase reporter vector fused with *NFE2L1*-3′UTR was transfected and cultured for 24 h. Control siRNA (siCont) was used as a control. Luciferase activity was normalized by mRNA levels of a *luciferase* gene. *, $P < 0.05$ ($n = 3$, means + SD, *t* test). (J) Impact of *NFE2L1*-3′UTR deletion or mutation on translation. The luciferase reporter vector fused with the indicated *NFE2L1*-3′UTR was transfected into HCT116 cells, and the cells were analyzed after 24 h. Luciferase activity was normalized according to the mRNA levels of a *luciferase* gene. Red and blue rectangles represent wild-type (WT) CPEs, which are highlighted in Fig. S3H, and an adenine-mutated CPE#2 (mCPE#2), respectively. **, $P < 0.01$; n.s., not significant ($n = 3$, means + SD, ANOVA followed by Tukey's test).

deletion did not (WT-Full versus WT-Δ#2–#5 or WT-Full versus WT-Δ#3–#5). The adenine mutation of CPE#2 (UUUUA→AAAAA) also induced translation via the full-length and CPE#3- to CPE#5-deleted *NFE2L1*-3′UTR (WT-Full versus mCPE#2-Full or WT-Δ#3–#5 versus mCPE#2-Δ#3–#5). These results clearly demonstrate that CPEB3 and CPE#2 in *NFE2L1*-3′UTR function as the *trans*-regulator and its *cis* element, which are involved in NFE2L3-mediated repression of NFE2L1 translation.

**CPEB3 is a key factor for maintaining basal proteasome activity and the poor prognosis of colorectal cancer patients.** We investigated the impact of *CPEB3* overexpression on the basal expression of proteasome-related genes, basal proteasome activity, and BTZ resistance. The basal mRNA levels of *PSMB3*, *PSMB7*, *PSMC2*, *PSMG2*, and *POMP* were not changed under single knockdown of *NFE2L3* (Fig. 4A and Fig. S4A and B, Emp + siCont versus Emp + siNFE2L3). Meanwhile, *CPEB3* overexpression significantly reduced these mRNA levels under single knockdown of *NFE2L3* (Fig. 4A and Fig. S4A and B, CPEB3 + siCont versus CPEB3 + siNFE2L3). Furthermore, *CPEB3* overexpression under *NFE2L3* single knockdown impaired the basal proteasome activity and the cancer cell resistance to BTZ (Fig. 4B and C and Fig. S4C). On the other hand, *CPEB3* overexpression under *NFE2L3* overexpression did not affect the expression levels of the proteasome subunit genes (Fig. S4D). Similarly, we observed no impact of *CPEB3* overexpression on BTZ resistance (Fig. S4E). We also found that the proteasome activity was not promoted by *CPEB3* knockdown under *NFE2L3* overexpression (Fig. S4F). We discuss these inconsistent results in Discussion.

Finally, we confirmed the clinical relevance of the current findings in colorectal cancer where both *NFE2L* genes are highly expressed. Using the data sets archived at The Cancer Genome Atlas, we confirmed that colorectal cancer patients with tumors expressing higher levels of *CPEB3*/*NFE2L3* exhibit shorter overall survival times but that higher *CPEB3*/*NFE2L1* expression is not associated with this (Fig. 4D and Fig. S5A). Interestingly, *CPEB3* mRNA levels are positively correlated with *NFE2L1* mRNA levels (Fig. S5B), implying that NFE2L1 increases its mRNA level to recover the reduction of its protein level by CPEB3 in colorectal cancer. On the other hand, we found no association with prognosis when analyzing colorectal cancer patients with high *CPEB3*/low *NFE2L1* expression and high *CPEB3*/high *NFE2L1* expression (Fig. S5C, top). However, high expression of *NFE2L3* is associated with poor prognosis of patients with high *CPEB3*/high *NFE2L1* levels (Fig. S5C, bottom). We also found a positive correlation between *NFE2L3* and *CPEB3* mRNA levels in several types of cancer, such as uveal melanoma (UVM) and the lymphoid neoplasm diffuse large B-cell lymphoma (DLBC) (Table S3).

These results clearly show that CPEB3 acts as a key factor for not only the complementary maintenance of basal proteasome activity in cancer cells by NFE2L1 and NFE2L3 but also the poor prognosis of cancer patients with high expression levels of *NFE2L3* but not *NFE2L1*.

## DISCUSSION

Here, we demonstrated the complementary, but not simultaneous, regulatory mechanism of basal proteasome activity in cancer cells through the NFE2L3-CPEB3-NFE2L1 translational repression axis (Fig. 4E). In cancer cells, NFE2L3 induces the basal expression of proteasome-related genes in parallel with NFE2L1 translational repression by inducing *CPEB3* gene expression (Fig. 4E, left). If *NFE2L3* gene expression is reduced, NFE2L1 escapes from the CPEB3-mediated translational repression and complementarily plays a transcriptional role for the robust maintenance of basal proteasome activity in cancer cells (Fig. 4E, right). Recent single-cell studies have provided important insights that the interaction between a transcription factor and the promoters are highly dynamic to create transcriptional profiles either in response to external signals or as a direct consequence of the internal molecular networks (17). This implies that NFE2L1 and NFE2L3 rapidly and robustly maintain the proteasome gene expression in response to proteasome inhibition by binding complementarily, but not competitively, to the promoters. We also found that NFE2L1 induces *CPEB3* gene expression (see Fig. S3G in the supplemental material) and that CPEB3 represses NFE2L1 translation (Fig. 3D

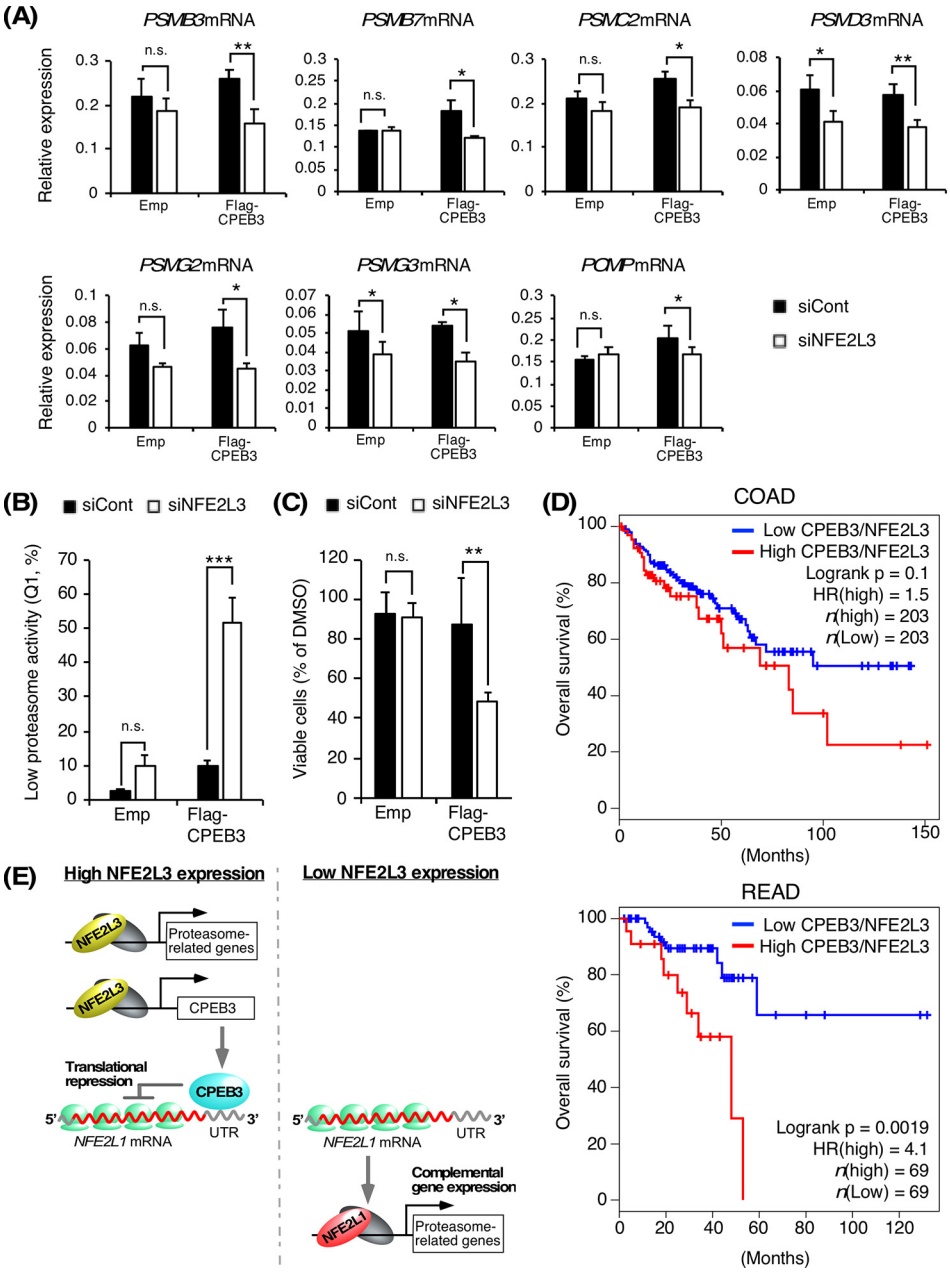


**FIG 4** NFE2L3 and CPEB3 contribute to maintain proteasome activity in cancer cells and the prognosis of colorectal cancer patients. (A to C) Impact of *CPEB3* overexpression under *NFE2L3* knockdown on the expression of the proteasome-related genes (A), proteasome activity (B), and BTZ resistance (C). HCT116 or ZsPS cells were used in panels A and C or in panel B, respectively. At 24 h after NFE2L3 siRNA transfection, the cells were additionally transfected with the 3×Flag-CPEB3 plasmid and cultured for 24 h. Control siRNA (siCont) and p3×FLAG-CMV 10 empty vector (Emp) without any fusion proteins were used as controls. In panel A, the cells were subjected to RT-qPCR using the primers for seven proteasome-related genes analyzed in Fig. 1C. mRNA levels of each proteasome subunit were normalized according to the levels of *β-actin* mRNA. In panel B, the fluorescence intensity derived from a ZsProSensor-1 reporter was measured using flow cytometry. The cell populations in Q1 enclosed by a red line are those with low proteasome activity. In panel C, the cells were treated with 10 nM BTZ and further incubated for 24 h. The cells then were subjected to cell viability assay using trypan blue staining. Cell viability was determined by the number of living cells with BTZ treatment normalized by that with DMSO. *, $P < 0.05$; **, $P < 0.001$; ***, $P < 0.005$; n.s., not significant ($n = 3$, mean + SD, *t* test). (D) Kaplan-Meier analysis comparing overall survival between groups expressing higher and lower levels of *CPEB3*/*NFE2L3*. The median values for *CPEB3* gene expression levels, normalized by *NFE2L3* gene expression levels, were used as the thresholds between tumors expressing higher and lower levels of *CPEB3*/*NFE2L3* or expressing higher and lower levels of *CPEB3*/*NFE2L1*, respectively. The hazard ratio (HR) was calculated based on Cox's proportional hazards model. Data are from patients having colorectal adenocarcinoma (COAD) or rectal adenocarcinoma (READ) from The Cancer Genome Atlas. (E) Schematic model of the mechanism of cross talk between NFE2L1 and NFE2L3 to complementarily maintain basal proteasome gene expression and activity in cancer cells through CPEB3-mediated translational repression.

and F). Although we have not yet confirmed whether NFE2L1 binds to the *CPEB3* promoter, we identified an NFE2L3-bound ARE in the *CPEB3* promoter (Fig. 3B). Considering that NFE2L1 and NFE2L3 bind to the ARE sequence, these results suggest the negative feedback regulation of NFE2L1 through CPEB3-mediated translational repression (Fig. S5D).

*NFE2L1* is ubiquitously expressed in normal tissues, and mice in which it is knocked out suffer embryonic lethality (18). Meanwhile, *NFE2L3* expression levels are low except in several tissues, such as the placenta (8), and *Nfe2l3* knockout mice do not exhibit any apparent abnormalities under normal physiological conditions (19–21). However, *NFE2L3* is highly expressed in many types of cancer cells, implying that the proteasome in cancer or normal cells is maintained through the NFE2L3-CPEB3-NFE2L1 translational repression axis or the negative feedback regulation of NFE2L1. Indeed, we revealed a clinical association of higher *CPEB3*/*NFE2L3* expression, but not higher *CPEB3*/*NFE2L1* expression, with poor prognosis of cancer patients (Fig. 4D; see also Fig. S5A in the supplemental material). Therefore, our findings suggest that while NFE2L1 maintains basal proteasome activity within an appropriate range for normal development, NFE2L3 adjusts the proteasome in terms of quality and quantity for cancer development.

We suggest that our findings have additional biological meanings for cancer. The functional difference between NFE2L3 and NFE2L1 is not in the regulation of the proteasome activity but rather in the expression of cancer-related genes, such as *VEGFA* (*Vascular Endothelial Growth Factor A*) and *DUX4* (*Double Homeobox 4*), which other groups have recently identified as NFE2L3-specific target genes (22, 23). Meanwhile, cancer cells have to keep NFE2L1 as a backup for proteasome regulation, because the proteasome activity is crucial for the more rapid proliferation of cancer cells (24). Thus, the NFE2L3-CPEB3-NFE2L1 translational repression axis enables cancer cells to grow more rapidly through NFE2L3-mediated signals and to maintain the proteasome activity through NFE2L1 immediately in case NFE2L3 does not work. Further study is needed to confirm this.

Unexpectedly, *NFE2L1* knockdown did not affect NFE2L3 protein levels (Fig. 2A and Fig. S2A), although *NFE2L1* knockdown reduced *CPEB3* mRNA levels (Fig. S3G) and the *NFE2L3* gene possessed several CPEs in its 3′UTR (blue highlighted numbers in Fig. S3H). CPEB3 belongs to the CPEB family, consisting of four paralogs, CPEB1, CPEB2, CPEB3, and CPEB4 (25). According to the binding RNA sequence, the CPEB family is functionally categorized into two groups, CPEB1 and CPEB2 to -4 (26), implying that CPEB2 and/or CPEB4 compensate for the reduction of the *CPEB3* gene by NFE2L1 depletion. An alternative possibility is a conversion of CPEB function in a cellular context-dependent manner (15). In maturing mouse and *Xenopus* oocytes, CPEB acts as a translational activator through phosphorylation by aurora kinase (27, 28). Therefore, there is an unknown mechanism of cross talk between the NFE2L and CPEB protein families.

Moreover, we showed that the proteasome activity was not promoted by *CPEB3* knockdown under *NFE2L3* overexpression (Fig. S4F). This result supports our conclusion that excessive NFE2L3 compensates for the impairment of proteasome activity if CPEB3 represses NFE2L1 translation. On the other hand, *CPEB3* overexpression under *NFE2L3* knockdown impaired proteasome-related gene expression and BTZ resistance (Fig. 4A and C and Fig. S4A to C), although *CPEB3* overexpression under *NFE2L3* overexpression did not (Fig. S4D and E), suggesting that the effect of *CPEB3* overexpression is masked by endogenous CPEB3. These results also imply unknown targets of CPEB3. The data in the literature are limited, and more investigations are needed to elucidate the definitive roles and target genes of CPEB3 in cancers, although those of CPEB4 have been extensively researched. For example, colorectal cancer tissues highly express *CPEB4*, and high *CPEB4* expression is correlated with advanced tumor stage, lymph node metastasis, distant metastasis, and poor prognosis in patients with colorectal cancers (29). In addition, RNA immunoprecipitation sequencing was performed, and *MITF*

(*microphthalmia-associated transcription factor*) was identified as a novel CPEB4 target gene in melanoma (30). Further study is needed to clarify this issue.

## MATERIALS AND METHODS

**Cell lines.** HCT116 (human colorectal carcinoma), T98G (human glioblastoma multiforme), and MCF-7 (human breast cancer) cells were cultured in Dulbecco's modified Eagle's medium (DMEM)-high glucose (Wako) supplemented with 10% fetal bovine serum (FBS; Nichirei), 40 $\mu$g/ml streptomycin, and 40 U/ml penicillin (Life Technology). H1299 (human non-small-cell lung cancer) cells were cultured in RPMI 1640 (Nacalai Tesque) supplemented with 10% FBS (Nichirei), 40 $\mu$g/ml streptomycin, and 40 U/ml penicillin (Life Technology). To generate the cells stably expressing a ZsProSensor reporter (ZsPS cells), HCT116 cells were transfected with the proteasome sensor vector (Clontech). To generate *NFE2L3*- and *GFP*-overexpressing cells, H1299 cells were transfected with the p3×FLAG-CMV 10 vector (Sigma-Aldrich) containing human full-length NFE2L3 or green fluorescent protein (GFP). The transfected cells were selected with G-418.

**Plasmid construction and mutagenesis.** The 3×Flag-CPEB3 plasmid was generated by subcloning the PCR-amplified human CPEB3 cDNA into the p3×FLAG-CMV 10 vector (Sigma-Aldrich). The human CPEB3 cDNA was synthesized using the following primers: forward, 5′-TTTGAATTCAATGCAGGATGATTTAC-3′; reverse, 5′-AAAGGATCCTCAGCTCCAGCGGAAC-3′. The luciferase reporter driven by *NFE2L1*-3′UTR-Full was generated by PCR amplification of human genomic DNA using the indicated primers (forward, 5′-GGCCGGCCGCCTGGGAAGAAGGGGGTT-3′; reverse, 5′-GGCCGGCCTTTTTTTTTTTTTTTTTTACAATGAGTCCA-3′) and cloned into pGL3-Control vector (Promega). The deletion of *NFE2L1*-3′UTR (*NFE2L1*-3′UTR-Δ#2-#5 or Δ#3-#5) was performed by a PCR-based method using the following primers: forward, 5′-TTTTTGGCCGGCCCCTGGGGAAGAAG-3′; reverse, 5′-TTTTTGGCCGGCCGACATTGTAGTCC-3′ (*NFE2L1*-3′UTR-Δ#2-#5) or 5′-TTTTTGGCCGGCCGCACTCCCAGGTT-3′ (*NFE2L1*-3′UTR-Δ#3-#5). The adenine mutation of CPE#2 in the *NFE2L1*-3′UTR was introduced by site-directed mutagenesis using PCR. The primer sequence was the following (altered nucleotides are underlined): 5′-ACAATGTCTTTATAAAAAACTGTTTGCCA-3′. All constructs were confirmed by sequencing.

**Antibodies.** The antibodies utilized in the current immunoblot analysis were anti-$\alpha$-tubulin (DM1A; Sigma-Aldrich), anti-NFE2L1 (D5B10; Cell Signaling Technology), anti-NFE2L3 (9408), anti-FLAG (M2; Sigma-Aldrich), and normal rabbit IgG (Wako). A monoclonal NFE2L3 antibody (9408) raised against human NFE2L3 (amino acids 364 to 415) was generated as described previously (14).

**Transfection.** The transfection of the plasmid DNA and short interfering RNA (siRNA) was performed using polyethylenimine (PEI) and RNAiMAX (Invitrogen), respectively. The sequences of the siRNA duplexes are listed in Table S4 in the supplemental material.

**RT-qPCR.** Total RNA was extracted and purified using ISOGEN II (Nippon Gene), in accordance with the manufacturer's instructions. Aliquots of total RNA (1 $\mu$g) were reverse transcribed using pd(N)6 random primer (TaKaRa Bio) and Moloney murine leukemia virus (M-MLV) reverse transcriptase (Invitrogen) with a deoxynucleoside triphosphate (dNTP; TaKaRa Bio) concentration of 250 $\mu$M, in accordance with the manufacturer's instructions. RT-qPCR was performed with SYBR Premix *Ex Taq* II (TaKaRa Bio) and primers for genes using a thermal cycler Dice real-time system (TaKaRa Bio). The expression level of each gene in human cells was normalized to the mRNA level of the human *β-actin* gene. qPCR primer sequences are described in Table S4.

**Immunoblot analysis.** To prepare whole-cell extracts, the cells were lysed with SDS sample buffer (50 mM Tris-HCl [pH 6.8], 10% glycerol, and 1% SDS). The protein quantities in cell extracts were measured with a bicinchoninic acid kit (ThermoFisher Scientific). The proteins were separated by SDS-PAGE and transferred to polyvinylidene difluoride membranes (Immobilon-P transfer membrane; EMD Millipore Corporation). After the membranes were blocked with Blocking One (Nacalai Tesque) at 4°C overnight, they were incubated with a primary antibody, washed with TBS-T (20 mM Tris-HCl [pH 7.6], 137 mM NaCl, 0.1% Tween 20), and incubated with a horseradish peroxidase-conjugated secondary antibody (Invitrogen). The blots were washed with TBS-T and developed with enhanced chemiluminescence (GE Healthcare).

**Cycloheximide chase experiments.** HCT116 cells were transfected with the indicated siRNA. At 48 h after transfection, the cells were treated with 20 $\mu$g/ml cycloheximide (CHX), and the whole-cell extracts were prepared at the indicated time points. The immunoblot analysis was conducted with the indicated antibodies. The cycloheximide chase assay results were depicted as fitted linear curves using GraphPad Prism 8.

**Protein synthesis assays.** The protein synthesis assays were conducted using the Click-iT Plus OPP protein synthesis assay kit (Invitrogen), in accordance with the manufacturer's protocol. HCT116 cells were transfected with the indicated siRNA. At 48 h after transfection, the cells were treated with *O*-propargyl-puromycin (OPP; 20 $\mu$M) for 1 h at 37°C and washed twice with phosphate-buffered saline (PBS). The cells were fixed using 4% paraformaldehyde for 15 min at room temperature, followed by washing them twice with PBS (containing 0.5% bovine serum albumin [BSA]) and then permeabilizing with PBSTx (0.5% Triton X-100–PBS) for 15 min at room temperature. The cells were washed twice with PBS (containing 0.5% BSA). After their treatment with Click-iT reaction mixtures for 30 min at room temperature in the dark, the cells were washed with Click-iT reaction rise buffer. Finally, the cells were washed with PBS and subjected to the protein synthesis assay using a BD FACSAria-II (Becton, Dickinson).

**Polysome fractionation assays.** HCT116 cells were treated with 100 $\mu$g/ml CHX in culture medium for 5 min at 37°C. The cells were washed twice with PBS containing CHX (100 $\mu$g/ml) and lysed with lysis buffer (15 mM Tris-HCl [pH 7.5], 300 mM NaCl, 25 mM EDTA, 1% Triton X-100, 0.5 mg/ml heparin, 100 $\mu$g/ml CHX) with 1× EDTA-free protease inhibitor cocktail (Nacalai Tesque). The lysate was centri-

fuged at 9,300 × *g* for 10 min at 4°C and loaded onto a linear 20% to 50% sucrose gradient buffer in 15 mM Tris-HCl [pH 8.0], 25 mM EDTA, and 300 mM NaCl. Centrifugation was conducted at 40,000 rpm for 2 h at 4°C in an SW-41 Ti rotor (Beckman Coulter), and fractions were collected from the top of the gradient (fractions 1 to 20). The RNA from each fraction was subjected to RT-qPCR analysis. The quantified mRNA was normalized by the input. qPCR primer sequences are described in Table S4.

**DNA microarray analysis.** Total RNA was processed with the Ambion WT expression kit (Affymetrix), in accordance with the manufacturer's instructions. cRNA was then fragmented, labeled, and hybridized to the Affymetrix human gene 1.0 ST arrays using the GeneChip WT terminal labeling and hybridization kit (Affymetrix). GeneChip Fluidics Station 450 was used for processing of the arrays, and fluorescent signals were detected with the GeneChip scanner 3000-7 G. Images were analyzed with the GeneChip operating software (Affymetrix).

The expression console and transcription analysis console (Affymetrix) were used to analyze the data. The PANTHER classification system with the theme "molecular function" was used for gene ontology analysis of the genes whose expression was reduced in siRNA-mediated *NFE2L3*-knockdown HCT116 cells (fold change, ≥1.4) and increased in stably *NFE2L3*-overexpressing H1299 cells (fold change, ≥1.4). The expression data of all genes in siRNA-mediated *NFE2L3*- or *NFE2L1*-knockdown HCT116 cells were subjected to GSEA using open-source software v3.0 (31) and the gene set containing 42 proteasome-related genes described in Table S1.

**ChIP qPCR and sequencing.** The cells were fixed with 1% formaldehyde for 10 min at room temperature, and then glycine was added to a final concentration of 0.125 M. The cells were lysed with cell lysis buffer (5 mM Tris-HCl [pH 8.0], 85 mM KCl, 0.5% NP-40) with protease inhibitors (Nacalai Tesque) and then centrifuged at 2,000 rpm and 4°C for 3 min. The pellets were further lysed with nuclear lysis buffer (50 mM Tris-HCl [pH 8.0], 10 mM EDTA, 1% SDS) with protease inhibitors (Nacalai Tesque), and the lysates were sonicated. After centrifugation at 15,000 rpm and 8°C for 10 min, the supernatants were collected. The supernatants then were diluted in ChIP dilution buffer (16.7 mM Tris-HCl [pH 8.0], 167 mM NaCl, 1.2 mM EDTA, 1.1% Triton X-100, 0.01% SDS). The diluted samples were precleared with 20 $\mu$l of Dynabeads protein G (ThermoFisher Scientific), and then the supernatants (used as an input sample) were incubated with anti-NFE2L3 or anti-NFE2L1 antibody. The immunocomplexes were collected by incubation with 20 $\mu$l of Dynabeads protein G (ThermoFisher Scientific) and then washed with the following buffers: low-salt wash buffer (20 mM Tris-HCl [pH 8.0], 150 mM NaCl, 2 mM EDTA, 1% Triton X-100, 0.1% SDS), high-salt wash buffer (20 mM Tris-HCl [pH 8.0], 500 mM NaCl, 2 mM EDTA, 1% Triton X-100, 0.1% SDS), and LiCl wash buffer (10 mM Tris-HCl [pH 8.0], 250 mM LiCl, 1 mM EDTA, 1% sodium deoxycholate, 1% NP-40). Finally, the beads were washed twice with 1 ml of TE buffer (10 mM Tris-HCl [pH 8.0], 1 mM EDTA). The immunocomplexes then were eluted by adding 200 $\mu$l of elution buffer (50 mM $NaHCO_3$, 1% SDS). After the reverse cross-linking by adding 200 mM NaCl, the remaining proteins were digested by adding proteinase K. For quantification of NFE2L3 binding to the target regions, RT-qPCR was performed using the purified DNA with the primers described in Table S4.

For ChIP sequencing, the libraries were prepared from 500 pg of immunoprecipitated DNA fragments using the KAPA Hyper Prep kit (KAPA Biosystems). The libraries were applied to single-end sequencing for 93 cycles on HiSeq2500 (Illumina). All sequence reads were extracted in FASTQ format using BCL2FASTQ Conversion Software 1.8.4 in the CASAVA 1.8.2 pipeline. Mapping was performed by BWA (version 0.5.9rc1) using the reference human genome, NCBI build 37 (hg19), and peak calling was conducted using MACS (version 1.4.2).

**RNA immunoprecipitation (RIP).** HCT116 cells were transfected with empty vector or 3×Flag-CPEB3 plasmid. At 48 h after transfection, cells were lysed in cell lysis buffer containing protease and RNase inhibitors. Lysates were sonicated for 10 min at low intensity and then precleared. Samples were immunoprecipitated using anti-FLAG antibody coupled to Dynabeads protein A (Invitrogen) for 3 h at 4°C. RNA bound to the FLAG beads was purified by phenol-chloroform extraction and subjected to RT-qPCR analysis. qPCR primer sequences are described in Table S4.

**Luciferase reporter assays.** Cells expressing the reporters indicated in the legends for Fig. 3H to J were lysed, and the luciferase activities were measured with the PicaGene luciferase assay system (Toyo Ink) and a microplate reader (Synergy HTX; BioTek Instruments).

**Proteasome activity analysis using a ZsProSensor reporter.** The ZsProSensor-1 protein is a fusion of the green fluorescent protein ZsGreen and mouse ornithine decarboxylase (MODC) and can be degraded by the proteasome without being ubiquitinated. ZsPS cells were transfected with the indicated siRNA or plasmid. The cells were collected at 48 h after transfection, followed by washing them twice with fluorescence-activated cell sorting (FACS) buffer (2% FBS in cold PBS). A total of 500 $\mu$l of FACS buffer containing 2 $\mu$g/ml propidium iodide (PI) was added to each sample. After their treatment at 4°C in the dark, samples were subjected to proteasome activity analysis using BD FACSAria-II (Becton, Dickinson).

***In vitro* proteasome activity assays.** *In vitro* proteasome activity assays were based on glycerol density gradient centrifugation and fluorogenic peptidase assays, as described previously (32). After centrifugation at 26,000 rpm for 22 h in a Beckman SW40Ti swing rotor, the gradient was manually separated into 20 fractions of 500 $\mu$l each. Since the 26S proteasome, which is made up of a 20S proteasome and one or two 19S-RPs, is contained in fractions 13 and 14, the mean fluorescence intensity was calculated as the proteasome activity with the following procedure: 30 $\mu$l of each fraction sample was transferred to a 96-well BD Falcon microtiter plate (BD Biosciences) and mixed with 2 mM ATP and 0.1 mM fluorogenic peptide substrate Suc-Leu-Leu-Val-Tyr-AMC (succinyl-Leu-Leu-Val-Tyr–7-amino-4-methylcoumarin; Peptide Institute). Fluorescence (380-nm excitation, 460-nm emission) was monitored on a microplate fluorometer (Synergy HTX; BioTek Instruments) every 5 min for 1 h (33).

**Cell viability assays using trypan blue staining.** HCT116 cells were transfected with siRNA and/or plasmid DNA under the conditions indicated in the legends for Fig. 1B and 4C and Fig. S1F, S4C, and S4E. After the treatment with 5 or 10 nM bortezomib (BTZ; Peptide Institute), the cells were stained with trypan blue and automatically counted using a TC20 automated cell counter (Bio-Rad Laboratories).

**Statistics and human cancer database.** Unpaired Student's *t* test was used to compare two groups, and one-way analysis of variance (ANOVA) followed by Tukey's *post hoc* test was used to compare multiple groups. GEPIA, a web server for cancer and normal gene expression profiling and interactive analyses (10), was used for Spearman's correlation, as shown in Fig. S5B and Table S3, and for Kaplan-Meier analyses, as shown in Fig. 4D and Fig. S5A. The median values for *CPEB3* gene expression levels normalized by *NFE2L3* or *NFE2L1* gene expression levels were used as the thresholds between tumors expressing higher and lower levels of *CPEB3*/*NFE2L3* or expressing higher and lower levels of *CPEB3*/*NFE2L1*, respectively (Fig. 4D and Fig. S5A). On the other hand, Kaplan-Meier analyses, as shown in Fig. S5C, were performed using expression and clinical data from 377 COAD specimens in TCGA PanCancer Atlas studies. Mean values and standard deviations (SD) of the mRNA levels of *NFE2L1*, *NFE2L3*, and *CPEB3* were calculated manually, and then each specimen was categorized into the high-expression group (greater than mean plus 0.5× SD) or the low-expression group (less than mean minus 0.5× SD). Kaplan-Meier survival curves were prepared using GraphPad Prism 8.

## SUPPLEMENTAL MATERIAL

Supplemental material is available online only.

**SUPPLEMENTAL FILE 1**, PDF file, 3.6 MB.

## ACKNOWLEDGMENTS

We thank Hiderori Watanabe, Mika Matsumoto, and Junko Naritomi for experimental support.

This work was supported in part by a Grant-in-Aid for Young Scientists (B) (17K18234 to T.W.), Grant-in-Aid for Scientific Research (C) (19K07650 to T.W.), The Uehara Memorial Foundation (to T.W.), Grant-in-Aid for Scientific Research (B) (16H03265 to A.K.), Grant-in-Aid for Challenging Research (Exploratory) (19K22826 to A.K.), and Grant-in-Aid for JSPS Fellows (18J20672 to A.H.).

T.W., H.K., and Y.T. conceived the project; T.W. and H.K. designed experiments; T.W., H.K., M.H., A.H., N.N., Y.T., N.T., and A.W. performed experiments and analyzed data; T.W. and A.K. wrote the manuscript; T.W. and A.K. provided funding; A.K. provided supervision.

We declare that we have no competing interests.

## REFERENCES

1. Adams J. 2003. The proteasome: structure, function, and role in the cell. Cancer Treat Rev 29:3–9. https://doi.org/10.1016/S0305-7372(03)00081-1.
2. Luo J, Solimini NL, Elledge SJ. 2009. Principles of cancer therapy: oncogene and non-oncogene addiction. Cell 136:823–837. https://doi.org/10.1016/j.cell.2009.02.024.
3. Radhakrishnan SK, Lee CS, Young P, Beskow A, Chan JY, Deshaies RJ. 2010. Transcription factor Nrf1 mediates the proteasome recovery pathway after proteasome inhibition in mammalian cells. Mol Cell 38:17–28. https://doi.org/10.1016/j.molcel.2010.02.029.
4. Tsuchiya Y, Taniguchi H, Ito Y, Morita T, Karim MR, Ohtake N, Fukagai K, Ito T, Okamuro S, Iemura S, Natsume T, Nishida E, Kobayashi A. 2013. The casein kinase 2-Nrf1 axis controls the clearance of ubiquitinated proteins by regulating proteasome gene expression. Mol Cell Biol 33:3461–3472. https://doi.org/10.1128/MCB.01271-12.
5. Sha Z, Goldberg AL. 2014. Proteasome-mediated processing of Nrf1 is essential for coordinate induction of all proteasome subunits and p97. Curr Biol 24:1573–1583. https://doi.org/10.1016/j.cub.2014.06.004.
6. Steffen J, Seeger M, Koch A, Krüger E. 2010. Proteasomal degradation is transcriptionally controlled by TCF11 via an ERAD-dependent feedback loop. Mol Cell 40:147–158. https://doi.org/10.1016/j.molcel.2010.09.012.
7. Lee CS, Lee C, Hu T, Nguyen JM, Zhang J, Martin MV, Vawter MP, Huang EJ, Chan JY. 2011. Loss of nuclear factor E2-related factor 1 in the brain leads to dysregulation of proteasome gene expression and neurodegeneration. Proc Natl Acad Sci U S A 108:8408–8413. https://doi.org/10.1073/pnas.1019209108.
8. Kobayashi A, Ito E, Toki T, Kogame K, Takahashi S, Igarashi K, Hayashi N, Yamamoto M. 1999. Molecular cloning and functional characterization of a new cap'n'collar family transcription factor Nrf3. J Biol Chem 274:6443–6452. https://doi.org/10.1074/jbc.274.10.6443.
9. Liu Y, Sethi NS, Hinoue T, Schneider BG, Cherniack AD, Sanchez-Vega F, Seoane JA, Farshidfar F, Bowlby R, Islam M, Kim J, Chatila W, Akbani R, Kanchi RS, Rabkin CS, Willis JE, Wang KK, McCall SJ, Mishra L, Ojesina AI, Bullman S, Pedamallu CS, Lazar AJ, Sakai R, Cancer Genome Atlas Research Network, Thorsson V, Bass AJ, Laird PW. 2018. Comparative molecular analysis of gastrointestinal adenocarcinomas. Cancer Cell 33:721–735. https://doi.org/10.1016/j.ccell.2018.03.010.
10. Tang Z, Li C, Kang B, Gao G, Li C, Zhang Z. 2017. GEPIA: a web server for cancer and normal gene expression profiling and interactive analyses. Nucleic Acids Res 45:W98–W102. https://doi.org/10.1093/nar/gkx247.
11. Adams J. 2004. The development of proteasome inhibitors as anticancer drugs. Cancer Cell 5:417–421. https://doi.org/10.1016/s1535-6108(04)00120-5.
12. Manasanch EE, Orlowski RZ. 2017. Proteasome inhibitors in cancer therapy. Nat Rev Clin Oncol 14:417–433. https://doi.org/10.1038/nrclinonc.2016.206.
13. Koizumi S, Irie T, Hirayama S, Sakurai Y, Yashiroda H, Naguro I, Ichijo H, Hamazaki J, Murata S. 2016. The aspartyl protease DDI2 activates Nrf1 to compensate for proteasome dysfunction. Elife 5:1–10. https://doi.org/10.7554/eLife.18357.
14. Chowdhury A, Katoh H, Hatanaka A, Iwanari H, Nakamura N, Hamakubo T, Natsume T, Waku T, Kobayashi A. 2017. Multiple regulatory mechanisms of the biological function of NRF3 (NFE2L3) control cancer cell proliferation. Sci Rep 7:12494. https://doi.org/10.1038/s41598-017-12675-y.
15. Fernández-Miranda G, Méndez R. 2012. The CPEB-family of proteins, translational control in senescence and cancer. Ageing Res Rev 11:460–472. https://doi.org/10.1016/j.arr.2012.03.004.
16. Afroz T, Skrisovska L, Belloc E, Guillén-Boixet J, Méndez R, Allain F. 2014. A fly trap mechanism provides sequence-specific RNA recognition by

CPEB proteins. Genes Dev 28:1498–1514. https://doi.org/10.1101/gad.241133.114.
17. Voss TC, Hager GL. 2014. Dynamic regulation of transcriptional states by chromatin and transcription factors. Nat Rev Genet 15:69–81. https://doi.org/10.1038/nrg3623.
18. Chan JY, Kwong M, Lu R, Chang J, Wang B, Yen TSB, Kan YW. 1998. Targeted disruption of the ubiquitous CNC-bZIP transcription factor, Nrf-1, results in anemia and embryonic lethality in mice. EMBO J 17:1779–1787. https://doi.org/10.1093/emboj/17.6.1779.
19. Derjuga A, Gourley TS, Holm TM, Heng HH, Shivdasani RA, Ahmed R, Andrews NC, Blank V. 2004. Complexity of CNC transcription factors as revealed by gene targeting of the Nrf3 locus. Mol Cell Biol 24:3286–3294. https://doi.org/10.1128/mcb.24.8.3286-3294.2004.
20. Kobayashi A, Ohta T, Yamamoto M. 2004. Unique function of the Nrf2-Keap1 pathway in the inducible expression of antioxidant and detoxifying enzymes. Methods Enzymol 378:273–286. https://doi.org/10.1016/S0076-6879(04)78021-0.
21. Chevillard G, Nouhi Z, Anna D, Paquet M, Blank V. 2010. Nrf3-deficient mice are not protected against acute lung and adipose tissue damages induced by butylated hydroxytoluene. FEBS Lett 584:923–928. https://doi.org/10.1016/j.febslet.2010.01.028.
22. Wang H, Zhan M, Yang R, Shi Y, Liu Q, Wang J. 2018. Elevated expression of NFE2L3 predicts the poor prognosis of pancreatic cancer patients. Cell Cycle 17:2164–2174. https://doi.org/10.1080/15384101.2018.1520558.
23. Bury M, Le Calvé B, Lessard F, Dal Maso T, Saliba J, Michiels C, Ferbeyre G, Blank V. 2019. NFE2L3 controls colon cancer cell growth through regulation of DUX4, a CDK1 inhibitor. Cell Rep 29:1469–1481. https://doi.org/10.1016/j.celrep.2019.09.087.
24. Loda M, Cukor B, Tam SW, Lavin P, Fiorentino M, Draetta GF, Jessup JM, Pagano M. 1997. Increased proteasome-dependent degradation of the cyclin-dependent kinase inhibitor p27 in aggressive colorectal carcinomas. Nat Med 3:231–234. https://doi.org/10.1038/nm0297-231.
25. Mendez R, Richter JD. 2001. Translational control by CPEB: a means to the end. Nat Rev Mol Cell Biol 2:521–529. https://doi.org/10.1038/35080081.
26. Huang YS, Kan MC, Lin CL, Richter JD. 2006. CPEB3 and CPEB4 in neurons: analysis of RNA-binding specificity and translational control of AMPA receptor GluR2 mRNA. EMBO J 25:4865–4876. https://doi.org/10.1038/sj.emboj.7601322.
27. Hodgman R, Tay J, Mendez R, Richter JD. 2001. CPEB phosphorylation and cytoplasmic polyadenylation are catalyzed by the kinase IAK1/Eg2 in maturing mouse oocytes. Development 128:2815–2822.
28. Mendez R, Hake LE, Andresson T, Littlepage LE, Ruderman JV, Richter JD. 2000. Phosphorylation of CPE binding factor by Eg2 regulates translation of c-mos mRNA. Nature 404:302–307. https://doi.org/10.1038/35005126.
29. Zhong X, Xiao Y, Chen C, Wei X, Hu C, Ling X, Liu X. 2015. MicroRNA-203-mediated posttranscriptional deregulation of CPEB4 contributes to colorectal cancer progression. Biochem Biophys Res Commun 466:206–213. https://doi.org/10.1016/j.bbrc.2015.09.008.
30. Pérez-Guijarro E, Karras P, Cifdaloz M, Martínez-Herranz R, Cañón E, Graña O, Horcajada-Reales C, Alonso-Curbelo D, Calvo TG, Gómez-López G, Bellora N, Riveiro-Falkenbach E, Ortiz-Romero PL, Rodríguez-Peralto JL, Maestre L, Roncador G, de Agustín Asensio JC, Goding CR, Eyras E, Megías D, Méndez R, Soengas MS. 2016. Lineage-specific roles of the cytoplasmic polyadenylation factor CPEB4 in the regulation of melanoma drivers. Nat Commun 7:13418. https://doi.org/10.1038/ncomms13418.
31. Subramanian A, Tamayo P, Mootha VK, Mukherjee S, Ebert BL, Gillette MA, Paulovich A, Pomeroy SL, Golub TR, Lander ES, Mesirov JP. 2005. Gene set enrichment analysis: a knowledge-based approach for interpreting genome-wide expression profiles. Proc Natl Acad Sci U S A 102:15545–15550. https://doi.org/10.1073/pnas.0506580102.
32. Murata S, Udono H, Tanahashi N, Hamada N, Watanabe K, Adachi K, Yamano T, Yui K, Kobayashi N, Kasahara M, Tanaka K, Chiba T. 2001. Immunoproteasome assembly and antigen presentation in mice lacking both PA28$\alpha$ and PA28$\beta$. EMBO J 20:5898–5907. https://doi.org/10.1093/emboj/20.21.5898.
33. Tanahashi N, Murakami Y, Minami Y, Shimbara N, Hendil KB, Tanaka K. 2000. Hybrid proteasomes. J Biol Chem 275:14336–14345. https://doi.org/10.1074/jbc.275.19.14336.